Hindawi
Journal of Advanced Transportation
Volume 2018, Article ID 1269439, 8 pages
https://doi.org/10.1155/2018/1269439

Research Article

A Dynamic Time Warping Algorithm Based Analysis of Pedestrian Shockwaves at Bottleneck

Lishan Sun[1], **Qingsheng Gong**[1], **Liya Yao**[2], **Wei Luo**[1] and **Tianqi Zhang**[1]

[1] *Beijing Key Laboratory of Traffic Engineering, Beijing University of Technology, 100 Pingleyuan, Chaoyang District, Beijing 100124, China*
[2] *School of Mechanical and Vehicular Engineering, Beijing Institute of Technology, 5 South Zhongguancun Street, Haidian District, Beijing 100081, China*

Correspondence should be addressed to Liya Yao; yaoliya@bit.edu.cn

Received 22 June 2017; Revised 29 September 2017; Accepted 16 November 2017; Published 9 January 2018

Academic Editor: Emanuele Crisostomi

Since the quantitative methodology analysis of the high-density pedestrian shockwaves at a bottleneck is limited, this paper proposes a dynamic time warping (DTW) algorithm for identifying, analyzing, and verifying the shockwaves. A set of real-world trajectory data is used to illustrate the proposed algorithm. Results show that the DTW algorithm is capable of depicting the pedestrian shockwaves elaborately and accurately. Results also show that the shockwave velocity is unsteady, as throughout time the gathering wave velocity and the evanescent wave velocity are decreasing and increasing, respectively. The mutual influence between followers and leaders is decreased when the shockwave spreads. There is a linear relationship between the shockwave velocity and density. Furthermore, singularities present a potential match solution to help identify the changing of pedestrian behaviors. The DTW algorithm for evaluating the pedestrian system stability has significant intrinsic features in the pedestrian traffic control and management.

1. Introduction

The rail transit, which has the advantages of high velocity, punctuality rate, and capacity, is the leading approach to solving traffic problems in cities with a large population; however, it has been getting overcrowded and uncomfortable for passengers inside the subway station. The design of pedestrian facilities for the rail transit needs to consider the complex behaviors of the pedestrian flows [1, 2]. In general, the design follows the rule of thumb (i.e., the designing rule with the assumption of ideal pedestrian behaviors), while it fails to reflect the actual pedestrian behaviors, causing potential security issues. Thus, the pedestrian behaviors in the pedestrian facilities with limited space capacity are worth studying.

The following is one of the most essential pedestrian behaviors. It may cause a pedestrian stampede, which occurs when large groups of people try to escape from confined spaces where escape path directions abruptly change. In the field of transportation, the following behavior of vehicles was first studied. Pipes [3] introduced the follow-the-leader concept based on the traffic flow theory. The optimal velocity model was then proposed to model the following behavior [4, 5]. Then Newell's car-following model was carried out to investigate the driving behavior with the trajectory data [6]. Based on Newell's car-following model, Taylor et al. [7] proposed Dynamic Time Warping (DTW) algorithm to examine driver heterogeneity in car-following behavior.

Since the pedestrian movements and vehicle movements are similar [6], the one-dimensional fluid dynamics model developed for the vehicle movements has been applied to the studies on pedestrian movements. For statistically investigating pedestrian flow, Lv et al. [8] analyzed the similarity between the vehicle following and the pedestrian following at the single lane and developed the optimal velocity model to study the pedestrian following behavior. Then, the social force model was calibrated and developed to simulate real-world scenarios in the pedestrian movement for evacuation scenarios, pilgrimage, and urban environments [9–11]. Support

Table 1: Position and velocity time-series data.

Time (s)		1	2	3	4	5	6	7
Leader	Position (m)	0.847	1.457	2.057	2.628	3.164	3.740	4.341
	Velocity (m/s)	1.455	1.475	1.300	1.135	1.083	1.217	1.417
Follower	Position (m)	−0.056	0.501	1.031	1.545	2.051	2.613	3.221
	Velocity (m/s)	1.013	1.211	1.096	1.006	1.071	1.190	1.749

Vector Machine (SVM) algorithm, cellular automata model, and normal cloud model have been created to reveal the pedestrian density-flow relationship and evaluate pedestrian dynamics following behavior in a subway station [12–17].

Being related to a pedestrian following behavior, the shockwave is a boundary in a pedestrian stream that represents a discontinuity in the flow-density domain [18]. Izadpanah et al. [19] proposed a new methodology to detect and analyze shockwaves based on traffic trajectory data. Li et al. [20] described the use of cloud-based crowdsourced probe data to simplify the problem of detecting the boundary of shockwaves between uncongested and congested conditions. Stanitsas and Hourdos [21] used shockwave activity as a surrogate of safety (shockwave length) and mobility (shockwave frequency) to evaluate shared hot lane facilities. Sundara et al. [22] analyzed the traffic shockwave propagation associated with darkness on highways and determined the value of darkness shockwave velocity propagation. Zhang et al. [23] proposed and verified the application and efficiency of a traffic shockwave model. Cho et al. [24] evaluate the shockwave effectiveness including theoretical verification based on traffic flow model and shockwave theory. However, the shockwaves, which often occur at the bottleneck, can quickly lead to congestion accidents. Since the quantitative methodology analysis of the high-density pedestrian shockwaves at bottleneck is limited, the accuracy and complexity of the velocity calculation of shockwave have not been studied. Hence, analysis of the pedestrian shockwave in detail at the bottleneck is needed.

This paper investigates the pedestrian movement at a bottleneck and presents a basic theory to evaluate the stability of the pedestrian system and have a great significance for the pedestrian traffic control and management. The main contribution of this paper is to propose a new approach, named DTW algorithm, for identifying, analyzing, and verifying the shockwaves. Compared with the fluid dynamic theory, the superiority of the DTW algorithm is that it provides a new method for calculating wave velocity using fewer parameters and simplified formula. This paper also contributes to using a set of real-world trajectory data to illustrate the proposed algorithm and validate the computational efficiency of the estimated results algorithm. The parameters, such as gathering wave velocity, the evanescent wave velocity, and the relationship between the shockwave velocity and the density, are analyzed.

2. Pedestrians following Characteristics

When pedestrians are compared with vehicles, pedestrians have more free and flexible behaviors and are more valuable to the influence of environment or other pedestrians. But behaviors of vehicles and pedestrians can still be considered to be similar. The pedestrian following movements in the single-file passageway is analogous to the vehicle following movements in the single lane. The leader is the person who influences a group of people into walking in a single-file passageway; the follower is the person who follows the leader walking in the single-file passageway. The movements of followers are all restricted by the leader and adjusted according to the positions and velocities of the leaders. The average velocity of the followers is less than or equal to the average velocity of the leaders so that collision is avoided. Vehicles or pedestrians are controlled by the conditions of space and velocity. The follower velocity is restricted by the space distance of the whole group. When the distance is decreased to a certain extent, vehicles or pedestrians must stop due to the congestion. Due to the existence of the reaction time, the change of motion of followers is always delayed after the change of motion of leaders. Due to the delay, the change of motion of the whole group at the bottleneck has a complex transfer phenomenon. We apply a follow model that has been developed for vehicle movement to the investigation of one-dimensional pedestrian movement.

3. DTW Algorithm

For the analysis of the pedestrian shockwave, the DTW algorithm is proposed that serves to extract the optimal match points and analyze pedestrian microscopic following behavior. Because of the advantage of matching precision, the DTW algorithm has been widely applied to the field of speech recognition, pattern recognition, and failure diagnosis [25–27] and the field of sensor technology for tracking pedestrian trajectories [28, 29]. The specific aim of this paper is to use the DTW algorithm to find the similarity or distance between pedestrian data sets.

The DTW algorithm is explained with an example of two-people trajectory data. The time-series data of position and velocity for the leaders and the followers are inputted and calibrated using SIMI Motion. Table 1 lists an example of the time input data.

A velocity difference matrix **C** is established to assess the cost of aligning each velocity data point in one-time series to all other points of the second time series, using the equation

$$C_{ij} = \sqrt{\left(x_i - y_j\right)^2} = \left|x_i - y_j\right|, \quad (1)$$

where x_i is the velocity of the leader at time point i and y_j is the velocity of the follower at time point j. An example of the velocity difference matrix is shown as follows:

$$\mathbf{C} = \begin{bmatrix} 0.442 & - & - & - & - & - & - \\ 0.462 & 0.264 & - & - & - & - & - \\ 0.287 & 0.089 & 0.204 & - & - & - & - \\ 0.122 & 0.076 & 0.039 & 0.129 & - & - & - \\ 0.070 & 0.128 & 0.013 & 0.077 & 0.012 & - & - \\ 0.204 & 0.006 & 0.121 & 0.211 & 0.146 & 0.027 & - \\ 0.404 & 0.206 & 0.321 & 0.411 & 0.346 & 0.227 & 0.332 \end{bmatrix}. \quad (2)$$

The velocity difference matrix **C** is used to calculate the cumulative velocity difference matrix **L** that denotes the cumulative least cost for continuously moving from the first pair to the last pair. The algorithm of the cumulative least cost evaluates the costs in the next cell vertically, horizontally, or diagonally away from the current cell in the matrix, using the equation

$$L_{ij} = C_{ij} + \min\left(L_{i-1,j-1}, L_{i-1,j}, L_{i,j-1}\right) \quad (i = 2, 3, \ldots, N;\ j = 2, 3, \ldots, M). \quad (3)$$

An example of the cumulative velocity difference matrix is shown as follows:

$$\mathbf{L} = \begin{bmatrix} 0 & - & - & - & - & - & - \\ 0.462 & 0.264 & - & - & - & - & - \\ 0.749 & 0.353 & 0.468 & - & - & - & - \\ 0.871 & 0.429 & 0.392 & 0.521 & - & - & - \\ 0.941 & 0.557 & 0.405 & 0.469 & 0.481 & - & - \\ 1.145 & 0.563 & 0.526 & 0.616 & 0.615 & 0.508 & - \\ 1.549 & 0.769 & 0.847 & 0.937 & 0.961 & 0.735 & 0.840 \end{bmatrix}. \quad (4)$$

The optimal alignment with the least cumulative velocity difference matrix, which starts at the last pair in the cumulative velocity difference matrix and works back to the first pair, is found. The warp path search pattern is used to search the next cell vertically, horizontally, and diagonally away from the current cell in the warp path. An example of the warp path is shown as follows (formatted in italics):

$$\begin{bmatrix} \mathit{0} & - & - & - & - & - & - \\ 0.462 & \mathit{0.264} & - & - & - & - & - \\ 0.749 & \mathit{0.353} & 0.468 & - & - & - & - \\ 0.871 & 0.429 & \mathit{0.392} & 0.521 & - & - & - \\ 0.941 & 0.557 & 0.405 & \mathit{0.469} & \mathit{0.481} & - & - \\ 1.145 & 0.563 & 0.526 & 0.616 & 0.615 & \mathit{0.508} & - \\ 1.549 & 0.769 & 0.847 & 0.937 & 0.961 & 0.735 & \mathit{0.840} \end{bmatrix}. \quad (5)$$

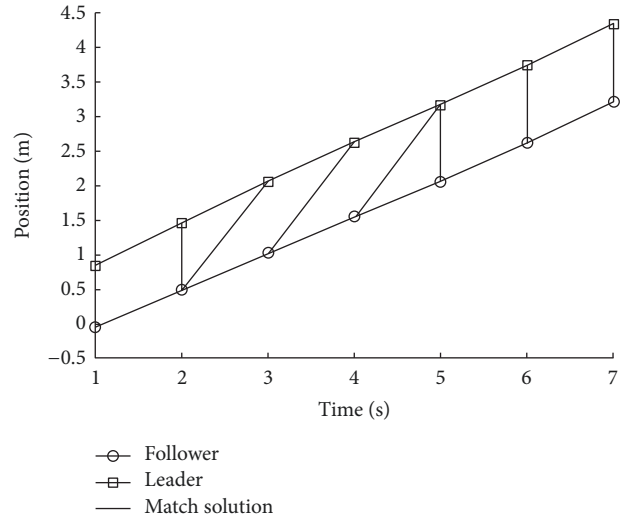

Figure 1: Pedestrian trajectories with DTW match solution.

When establishing the warp path, one potential problem arises when the values of the cumulative velocity differences in the adjacent cells are equal. Thus, a prespecified warp path step direction (diagonal step is preferred) is specified to help guide the algorithm through the cumulative velocity difference matrix.

The DTW algorithm (programmed using MATLAB) is applied to intuitively and precisely find the optimal corresponding between two timestamps. Note that the algorithm allows one-to-many matching in time series. An example of the matching result is shown in Figure 1 (the position data is shown in Notations and Input Parameters).

4. Analysis of the Shockwaves with Practical Pedestrian Behavior Data

4.1. Data Collection. A bottleneck typically denotes a narrowed area that reduces the flow through a channel. For identifying and analyzing the shockwave characteristics of a pedestrian in subway bottleneck, 300 shockwave samples were collected by the videos of two peak hours at 10 typical bottlenecks in Beijing subway stations. The videos are processed by the SIMI Motion software to obtain data of parameters such as velocity and position of pedestrians. Then, a MATLAB program is developed to perform DTW calculations and visualizations.

4.2. The Identification of Shockwaves. One typical bottleneck is selected as an example to illustrate the identifying process of shockwave using DTW algorithm, as shown in Figure 2(a) (the scene before the bottleneck is selected). Figure 2(b) shows the optimal matching results through the DTW algorithm. For evaluating the shockwave transmitting, the data for the blank group is collected from subway channel. Figures 3(a) and 3(b) show the scene and the optimal matching results. A phenomenon of shockwave transmission in multiple locations along the trajectory at the bottleneck is

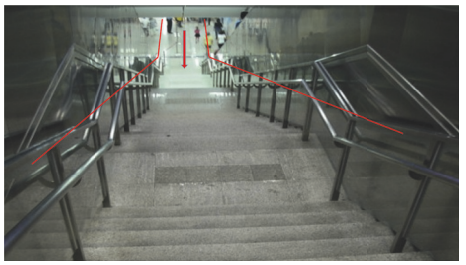

(a) The scene of the bottleneck

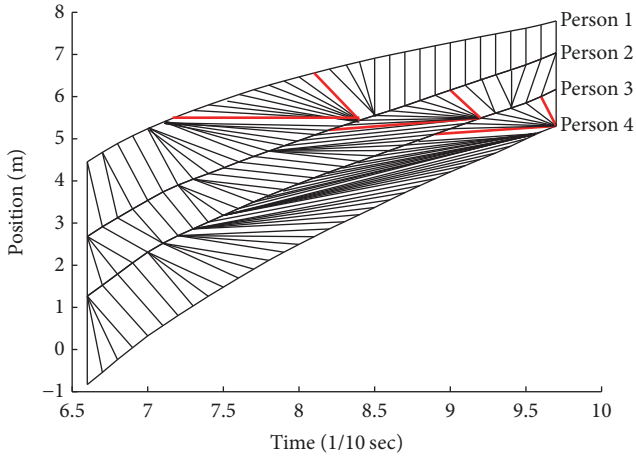

(b) The matching results of bottleneck

Figure 2: The matching results in bottleneck using DTW algorithm.

(a) The scene of no bottleneck

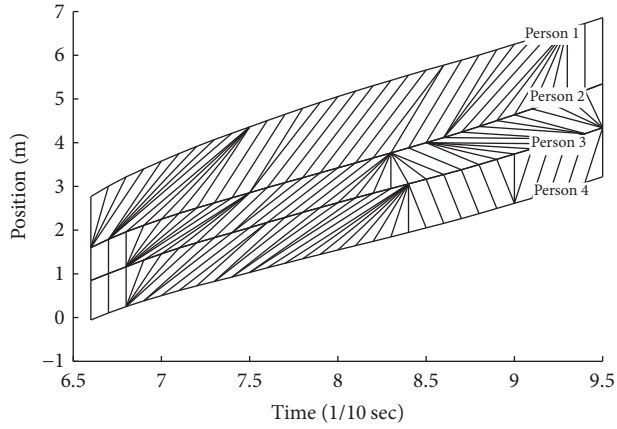

(b) The matching results of blank group

Figure 3: The matching results in channel using DTW algorithm.

identified by comparing with the blank group (which present a parallel matching line).

The shockwave velocity is defined as the slope of the optimal matching line between two points and is a primary parameter of depicting the characteristics of shockwaves. Figure 4 visualizes the key points highlight in matching results, and Table 2 lists the values of the key parameters. The optimal match point coordinate obtained through the DTW algorithm is extracted to analyze pedestrian following parameters. There is a phenomenon of shockwave transmission when pedestrians walk through the bottleneck. Lines AB, CD, and EF are the boundaries between low-density state and high-density state, indicating the tendency of gathering. On the contrary, lines GB, HD, and IF are the boundaries from high-density state to low-density state, indicating the tendency of dissipating.

In Table 2, since $k_{AB} > k_{CD} > k_{EF}$, the shockwave velocity appears to change in the entrance and departure regions, a slight trend toward decreasing before congestion and increasing congestion. Meanwhile, since $|k_{GB}| < |k_{HD}| < |k_{IF}|$ and $S_{\Delta ABG} > S_{\Delta CDH} > S_{\Delta EFI}$, the evanescent wave velocity increases gradually, and the influence decreases gradually.

4.3. The Verification of Shockwaves. The fluid dynamic theory is introduced to verify the shockwaves identification results of DTW algorithm. The velocity of shockwave is calculated using

$$\begin{aligned} W &= \frac{Q_1 - Q_2}{K_1 - K_2} \\ K &= \frac{1}{l} \\ Q &= vK = \frac{v}{l} \\ W &= \frac{Q_1 - Q_2}{K_1 - K_2} = \frac{v_1/l_1 - v_2/l_2}{1/l_1 - 1/l_2} = \frac{l_2 v_1 - l_1 v_2}{l_2 - l_1}, \end{aligned} \tag{6}$$

Table 2: Value of the key parameter.

Key point	Time (s)	Position (m)	Wave velocity (m/s)	Triangle area S (m^2)
A	7.2	5.035		
B	8.5	5.551		
C	8.2	5.207		
D	9.2	5.489	$k_{AB} = +0.397$ $k_{GB} = -1.272$	$S_{\Delta ABG} = 0.434$
E	8.9	5.108	$k_{CD} = +0.282$ $k_{HD} = -3.330$	$S_{\Delta CDH} = 0.361$
F	9.7	5.304	$k_{EF} = +0.245$ $k_{IF} = -6.960$	$S_{\Delta EFI} = 0.287$
G	8.1	6.060		
H	9.0	6.155		
I	9.6	6.000		

Table 3: Values of pedestrian shockwaves.

Transfer direction	Gathering wave velocity (m/s)	Evanescent wave velocity (m/s)
$v_1(1 \rightarrow 2)$	0.550	0.921
$v_2(2 \rightarrow 3)$	0.401	2.685
$v_3(3 \rightarrow 4)$	0.261	5.246

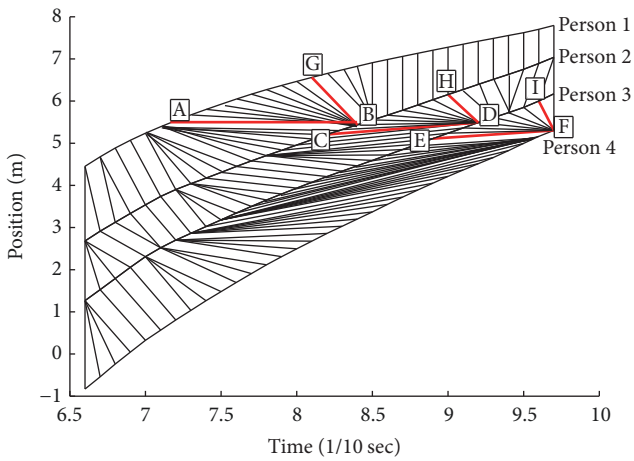

Figure 4: Key points highlight in matching results.

where the parameter W is the velocity of shockwave, Q_1, Q_2 are the pedestrian flow in a different state, K_1, K_2 are the pedestrian density in different state, v_1, v_2 are the pedestrian velocity in different state, and l_1, l_2 are the pedestrian distance in a different state.

Table 3 lists the change of the shockwaves velocity. Figure 5 presents the comparison of the two algorithms for gathering and evanescent wave. The tendency of the shockwave velocity changing between the two algorithms is consistent, which verifies the analysis of the phenomenon of shockwaves by using the DTW algorithm. Compared with the fluid dynamic theory, the superiority of the DTW algorithm is more intuitively and precisely finding the changing point of wave velocity; on the other hand, it provides a new method of calculating wave velocity. Fewer parameters and more straightforward formula are beneficial to reduce the complexity of calculation.

5. The Shockwaves Characteristics of Pedestrian Flow

The typical shockwaves parameters of pedestrian flows, such as singularities, shockwave velocity, and density, are further analyzed using the 25 groups of pedestrian trajectory data.

5.1. Singularity Analysis. Relevant to the shockwave characteristics of the pedestrian flow, the singularity occurs where a large section of time series is matched with a single point in the other time series.

The physics of the singularity in the pedestrian crowd is the pedestrian's speed variation, which affects the stability of the pedestrian system. Singularities are divided into two types: the follower's reaction is mapped to multiple actions by the leader (which present equilateral triangle); the multiple actions by the follower are mapped to a single action by the leader (which present inverted triangle), as shown in Figure 6.

The singularities offer a matching solution which is presenting a new perspective identifying pedestrian following behavior. The size of the angle θ at the singularity has an important implication for the individual pedestrian following behavior of shockwaves. Different angles indicate that the individual reaction time for state changes diverges. At bottleneck, especially in a high density of pedestrian, as the angle increases, the follower reaction time increases, and the pedestrian flow state is increasingly unstable.

5.2. Evaluation of the Parameters of Density and Shockwave Velocity in Pedestrian Flow. The relationship between the density and shockwave velocity of pedestrian flow is analyzed. The changing shockwaves velocity is obtained, as shown in Figure 7. The gathering wave velocity decreased due to the limited capacity and disappeared at the end, while the evanescent wave velocity increased reversely. Both the gathering wave velocity and the evanescent wave velocity have a close linear relationship, as shown in Table 3.

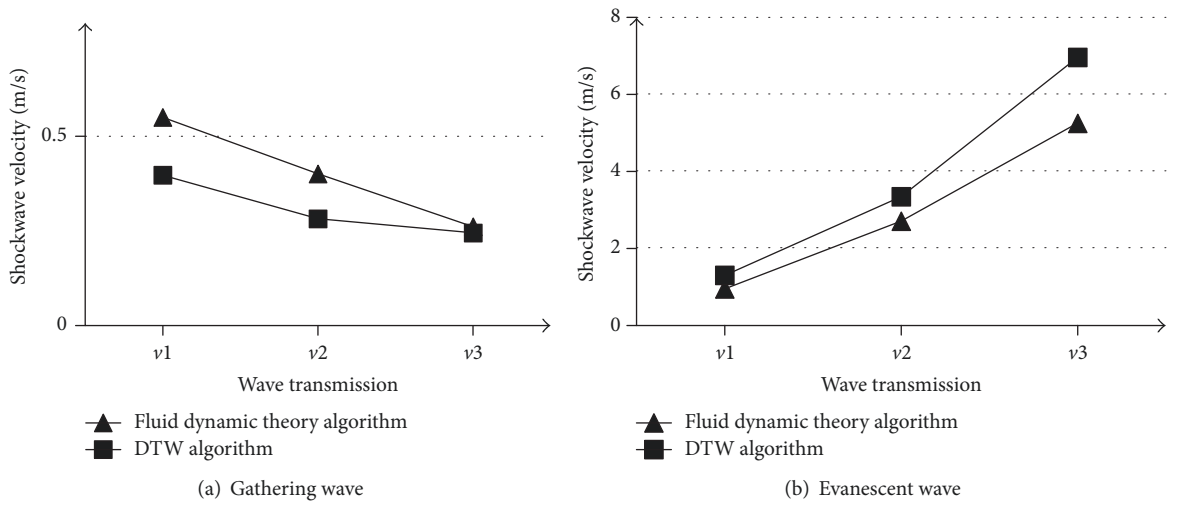

FIGURE 5: Comparison of the two algorithms for gathering and evanescent wave.

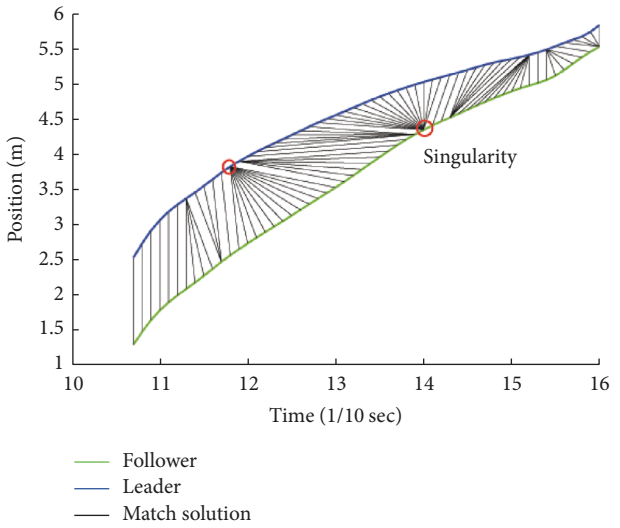

FIGURE 6: Example output for DTW pedestrian data match with highlighted singularity.

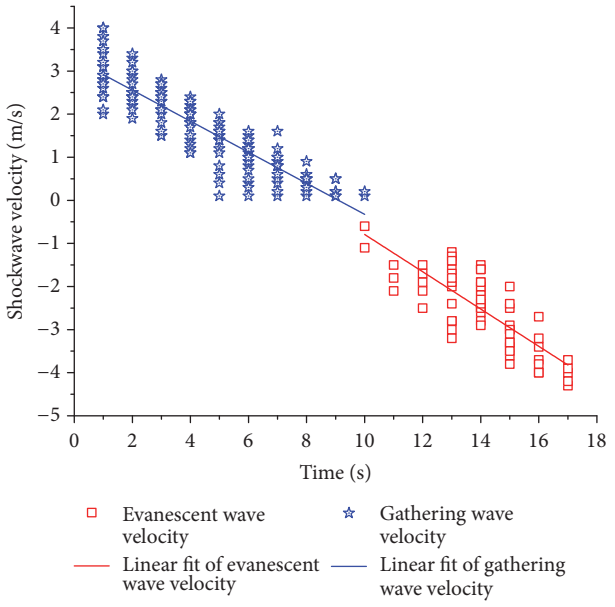

FIGURE 7: Shockwave velocity for 25 times of pedestrian flow.

Figure 8 shows the changing density of the pedestrian flow. The density of the pedestrian flow increases before the bottleneck happens and decreases after that, which presents a phenomenon of "low density-high density-low density." For the pedestrian psychology of escaping from the crowd, the acceleration of pedestrian after bottleneck is larger than the one before the bottleneck happens. Also, the density of the pedestrian flow has a quadratic correlation, as shown in Table 4.

Results show an intimate relationship between the shockwave velocity and the density (Figure 9). The shockwave velocities, including both gathering wave velocity and evanescent wave velocity, decrease with the density increase. The evanescent wave velocity has a larger acceleration than gathering wave velocity, which results from the psychology of pedestrian escaping from the crowd. Moreover, there is a linear relationship between the density and either the gathering wave velocity or the evanescent wave velocity.

6. Conclusion

The DTW algorithm is capable of identifying, analyzing, and verifying the shockwaves of pedestrians using the crowd trajectory data in traffic bottleneck. Compared with the fluid dynamic theory, the superiority of the DTW algorithm is that it provides a new method of calculating wave velocity. Fewer parameters and more simple formula are beneficial to reduce the complexity of calculation. The parameters, such as gathering wave velocity, the evanescent wave velocity,

Table 4: Values of density and shockwaves velocity of pedestrian Flow.

Shockwaves velocity/density	Mean	Max	Min	Std	Fitting analysis	R^2
Gathering wave velocity	1.5	4	0.1	0.97	$y = -0.36x + 3.28$	0.83
Evanescent wave velocity	2.5	4.3	0.6	0.87	$y = -0.43x + 3.53$	0.71
Density	2.4	4	1	0.70	$y = -0.03x^2 + 0.61x + 0.48$	0.81
Gathering velocity-density	-	-	-	-	$y = -1.01x + 4.00$	0.80
Evanescent velocity-density	-	-	-	-	$y = 1.37x - 5.71$	0.81

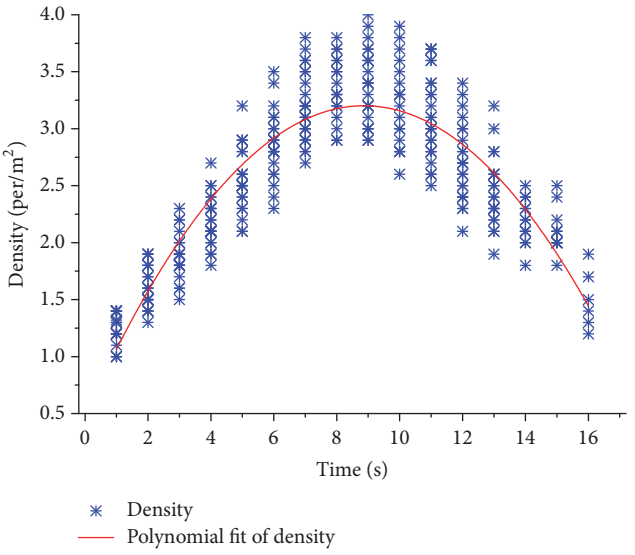

Figure 8: Density for 25 times of pedestrian flow.

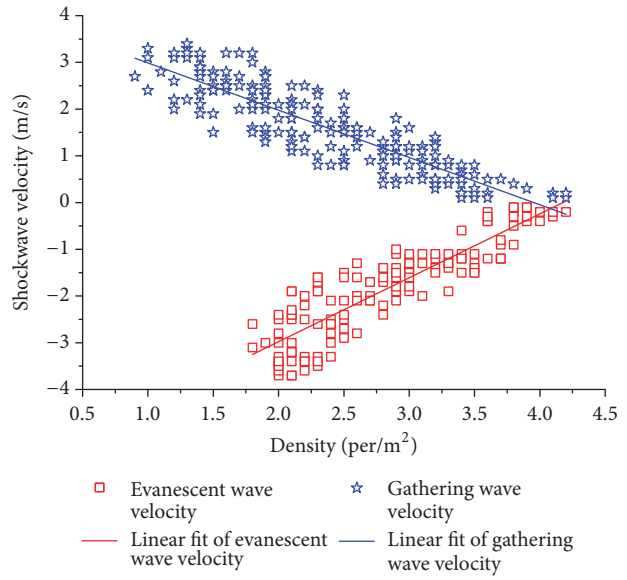

Figure 9: Relationship between shockwave velocity and density.

and the relationship between the shockwave velocity and the density, are also analyzed. Results show that there is a linear relationship between the shockwave velocity and the density. Also, a set of real-world trajectory data is used to illustrate the proposed algorithm and validate the computational efficiency of the estimated results algorithm. The DTW algorithm for evaluating the pedestrian system stability has significant intrinsic features in the pedestrian traffic control and management.

Notations and Input Parameters

k_i: The slope of the line i
S_Δ: The area of triangle
θ: The response sensitivity of pedestrian state changes
$\mathbf{C}$: The velocity difference matrix
x_i: The velocity of the leader at different time points i
y_j: The velocity of the follower at different time points j
$\mathbf{L}$: The cumulative velocity difference matrix
W: The velocity of shockwave
Q_i: The pedestrian flow in state i
K_i: The pedestrian density in state i
v_i: The pedestrian velocity in state i
l_i: The pedestrian distance in state i.

Conflicts of Interest

The authors declare that there are no conflicts of interest regarding the publication of this paper.

Acknowledgments

The authors would like to acknowledge the financial support for this study provided by the National Natural Science Foundation of China (no. 51308017), Beijing Nova Program (Grant no. Z141106001814110), Science and Technology Program of Beijing (Grant no. D161100005616001), and Ministry of Housing and Urban Construction in 2016 Science and Technology Project Plan (no. 2016K8044). The authors also would like to thank Dr. Xuesong Zhou for the algorithm improvement which helped us substantially improve this paper.

References

[1] L. Sun, W. Luo, L. Yao, S. Qiu, and J. Rong, "A comparative study of funnel shape bottlenecks in subway stations," *Transportation Research Part A Policy & Practice*, vol. 98, pp. 14–27, 2017.

[2] L. Sun, S. Hao, Q. Gong, S. Qiu, and Y. Chen, "Pedestrian roundabout improvement strategy in subway stations," *Transport*, pp. 1–10, 2017.

[3] L. A. Pipes, "An operational analysis of traffic dynamics," *Journal of Applied Physics*, vol. 24, no. 3, pp. 274–281, 1953.

[4] M. Bando, K. Hasebe, A. Nakayama, A. Shibata, and Y. Sugiyama, "Dynamical model of traffic congestion and numerical simulation," *Physical Review E: Statistical, Nonlinear, and Soft Matter Physics*, vol. 51, no. 2, pp. 1035–1042, 1995.

[5] D. Helbing and B. Tilch, "Generalized force model of traffic dynamics," *Physical Review E Statistical Physics Plasmas Fluids & Related Interdisciplinary Topics*, vol. 58, no. 1, pp. 133–138, 1998.

[6] G. Newell, "A simplified car-following theory: a lower order model," *Transportation Research Part B: Methodological*, vol. 36, no. 3, pp. 195–205, 2002.

[7] J. Taylor, X. Zhou, N. M. Rouphail, and R. J. Porter, "Method for investigating intradriver heterogeneity using vehicle trajectory data: a dynamic time warping approach," *Transportation Research Part B Methodological*, vol. 73, pp. 59–80, 2015.

[8] W. Lv, Z. Fang, X. Wei, W. Song, and X. Liu, "Experiment and modelling for pedestrian following behavior using velocity-headway relation," *Procedia Engineering*, vol. 62, pp. 525–531, 2013.

[9] D. Helbing, I. Farkas, and T. Vicsek, "Simulating dynamical features of escape panic," *Nature*, vol. 407, no. 6803, pp. 487–490, 2000.

[10] T. Werner and D. Helbing, "The social force pedestrian model applied to real life scenarios," *Pedestrian and Evacuation Dynamics*, vol. 3, 2003.

[11] A. Johansson, D. Helbing, and P. K. Shukla, "Specification of the social force pedestrian model by evolutionary adjustment to video tracking data," *Advances in Complex Systems*, vol. 10, Supplement 2, pp. 271–288, 2007.

[12] W. Zeng, P. Chen, H. Nakamura, and M. Iryo-Asano, "Application of social force model to pedestrian behavior analysis at signalized crosswalk," *Transportation Research Part C: Emerging Technologies*, vol. 40, pp. 143–159, 2014.

[13] Y. W. Chen, X. D. Cheng, H. Yang, X. G. Wang, and H. P. Zhang, "Pedestrian detection based on intelligent video of subway station," *Fire Safety Science*, vol. 22, no. 2, pp. 102–106, 2013.

[14] X.-X. Jian, S. C. Wong, P. Zhang, K. Choi, H. Li, and X. Zhang, "Perceived cost potential field cellular automata model with an aggregated force field for pedestrian dynamics," *Transportation Research Part C: Emerging Technologies*, vol. 42, pp. 200–210, 2014.

[15] Y. Wei, Q. Tian, and T. Guo, "An improved pedestrian detection algorithm integrating haar-like features and HOG descriptors," *Advances in Mechanical Engineering*, vol. 2013, Article ID 546206, 2013.

[16] G. Lämmel, H. J. Park, and J. Zhang, "Pedestrian Modeling using Cellular Automata Approach for Urban Street Facility: A Case Study in vicinity of Grand Central Terminal, New York City 2," in *Proceedings of the Transportation Research Board 95th Annual Meeting*, 2016, (No. 16-0698), https://www.researchgate.net/publication/292397830.

[17] J. B. Zhou, H. Chen, and B. Yan, "Identification of Pedestrian Crowding Degree in Metro Transfer Hub Based on Normal Cloud Model," *Journal of Jilin University (Engineering and Technology Edition)*, vol. 46, no. 1, pp. 100–107, 2016.

[18] A. D. May, *Traffic Flow Fundamentals*, Prentice Hall, Upper Saddle River, NJ, USA, 1990.

[19] P. Izadpanah, B. Hellinga, and L. Fu, "Automatic traffic shockwave identification using vehicles' trajectories," in *Proceedings of the 88th Annual Meeting of the Transportation Research Board (CD-ROM)*, 2009.

[20] H. Li, S. M. Remias, C. M. Day, M. M. Mekker, J. R. Sturdevant, and D. M. Bullock, "Shock wave boundary identification using cloud-based probe data," *Transportation Research Record*, vol. 2526, pp. 51–60, 2015.

[21] P. D. Stanitsas and J. Hourdos, "Simulating Realistic Shockwave Propagation on HOT Lanes," in *Proceedings of the Transportation Research Board 92nd Annual Meeting*, 2013.

[22] P. Sundara, O. C. Puan, and M. R. Hainin, "Determining the impact of darkness on highway traffic shockwave propagation," *American Journal of Applied Sciences*, vol. 10, no. 9, pp. 1000–1008, 2013.

[23] X. Zhang, J. Wu, and Y. Du, "The study of critical nodes of road network based on traffic shockwave model," in *Proceedings of the International Conference on Computing and Convergence Technology*, pp. 102–107, 2013.

[24] R. H. Cho, C. Y. Kim, and E. P. Ji, "Theoratical verification of VSL based on traffic flow model and shock wave theory," in *Proceedings of the Eastern Asia Society for Transportation Studies*, 2010.

[25] H. L. Le, N. T. Hai, N. V. Thuyen, T. T. Mai, and V. V. Toi, "MFCC-DTW Algorithm for Speech Recognition in an Intelligent Wheelchair," in *Proceedings of the 5th International Conference on Biomedical Engineering in Vietnam*, 2015.

[26] J. Galbally and D. Galbally, "A pattern recognition approach based on DTW for automatic transient identification in nuclear power plants," *Annals of Nuclear Energy*, vol. 81, pp. 287–300, 2015.

[27] C. H. Hwang, Y. M. Kim, C. H. Kim, and J. M. Kim, "Fault detection and diagnosis of induction motors using lpc and dtw methods," *Journal of the Korea Society of Computer and Information*, vol. 16, no. 3, pp. 141–147, 2011.

[28] Y. Li, Y. Zhuang, H. Lan, P. Zhang, X. Niu, and N. El-Sheimy, "Self-Contained Indoor Pedestrian Navigation Using Smartphone Sensors and Magnetic Features," *IEEE Sensors Journal*, vol. 16, no. 19, pp. 7173–7182, 2016.

[29] W. Liu, Y. Zhang, and X. Yang, "Pedestrian navigation using inertial sensors and altitude error correction," *Sensor Review*, vol. 35, no. 1, pp. 68–75, 2015.